 doi:10.20944/preprints202209.0052.v1

Article

Study on the Microstructure Evolution and Strength Damage Mechanism of Dolomite under Dissolution Condition

Wenlian Liu [1], Pengen Liu [2,*], Hanhua Xu [1], Bocheng Gong [2] and Feng Ji [2]

[1] Kunming Prospecting Design Institute of China Nonferrous Metals Industry, Kunming, Yunnan 650051, China; lwenl702@sina.com (W.L.); 724767210@qq.com (H.X.)
[2] State Key Laboratory of Geohazard Prevention and Geo-environment Protection, Chengdu University of Technology, Chengdu 610059, China; 1305238035@qq.com (B.G.); jeifens@163.com (F.J.)
* Correspondence: 1667671098@qq.com; Tel.: +86-17866535823

Abstract: Dolomite is a common type of natural soluble rock. The strength of rock decreases under the action of corrosion, which has a significant impact on the self-stability and long-term safety of the tunnel surrounding the rock. To reveal the microscopic structure evolution and strength-damage law of carbonate rock caused by chemical corrosion, a series of tests such as rock chemical corrosion test, rock uniaxial compression test, and electron microscope scanning test are conducted at different pH values on the dolomite of the Doushantuo Formation. The rock dissolution at different pH values exhibits four typical stages: the initial dissolution stage, secondary dissolution acceleration stage, stable dissolution rate stage, and dissolution attenuation stage. During the dissolution process, the initial dissolution rate is 25.91 times that of the stable stage, and the maximum strength attenuation is 76.2% after 21 days of dissolution. For macroscopic failure, the rock is developed from 1 to 2 external fractures to multiple internal and external fractures and penetrated, and the specimen transforms from brittle to flexible. For microstructure, the sample exhibits corrosion characteristics along the joint surface, intensified corrosion at the edge, etc. The porosity increase rate is 0.6%/d; however, the length–width ratio of the pores is maintained at 1.7–1.85, indicating that the development rate of pores in different directions is similar. The results of this study have enriched the study of the dolomite dissolution mechanism and have important reference value for the stability evaluation of tunnel surrounding rock in karst environments.

Keywords: dolomite; dissolution rate; time scale; quantitative analysis; microstructure; intensity attenuation

1. Introduction

In engineering construction in karst development areas, all types of karst engineering geological problems are encountered, such as reservoir and dam karst leakage, karst dam foundation, and slope problems. The karst sanding of dolomite decreases the strength of rock mass, reduces the quality of rock mass, and significantly affects the stability of slopes and underground chambers as unfavorable geological boundaries [1–3]. Therefore, the study of various properties under the dissolution conditions of dolomite is extremely important, and Wiederhorn et al. [4] have studied the influence of pH on glass crack propagation as early as 1973. Atkinson et al. [5] have experimentally studied the influence of HCl and NaOH solutions on the crack propagation rate, stress intensity factor, and stress intensity factor of quartz materials. Tang et al. [6] have discussed the methods for quantitatively analyzing rock water chemical damage and proposed and analyzed the hierarchical zoning of rock water chemical damage. Feng et al. [7] have defined the chemical damage factor by considering the initial pH value and time using the chemical reaction rate equation and measuring the change in the pH value of the solution during the soaking process. Cui et al. [8] and Huang et al. [9] have pointed out that the dissolution degree and dissolution rate of carbonate karst increase with an increase in temperature, according to the experimental results of dissolution kinetics. Xie [10], Yurtdas [11], and Li et al. [12]

 doi:10.20944/preprints202209.0052.v1

have analyzed the influence of chemical corrosion on rock strength. Wang et al. [13] have conducted corrosion tests on red sandstone using different chemical solutions and obtained the change rule of sample relative mass and solution pH value in the soaking process. Deng et al. [14] have used continuous damage mechanics and statistical theory to couple the damage effects of the immersion-drying cycle of water-rock to the damage statistical constitutive model. The influence of the compact section is emphasized, and the constitutive equation of the statistical damage of sandstone under the action of water-rock is established in segments. Chen et al. [15] have used computed tomography (CT) technology to analyze the mesoscopic mechanism of sandstone damage evolution and established a damage variable model based on the influence of chemical corrosion and CT number.

Additionally, the simulated dissolution tests of rocks indoors and the study of mesoscopic structures are important. The dissolution experiments of carbonate rocks under simulated stratigraphic conditions have been carried out by domestic and foreign scholars [16–20]. Kuva et al. [21] have used a chemical solution to soak the rock at different times, with X-ray tomography and scanning electron microscopy (SEM), to determine the microscopic pore structure of the rock. She et al. [22], based on a quantitative comparison of the changes in pore volume and permeability before and after dissolution and the pore evolution inside the rock, have pointed out that the pore structure controls the erosion effect and dissolution pore evolution of carbonate karst.

However, the qualitative and quantitative analysis of the evolution of dolomite dissolution microstructure is insufficient, and research on the characteristics and mechanical strength damage in different dissolution environments are not sufficient and comprehensive. In this study, based on previous studies, the above problems are comprehensively studied using an indoor chemical dissolution test, the SEM observation of microscopic structure, pores and cracks analysis system (PCAS), the quantitative analysis of microscopic parameters, and a uniaxial compressive strength test. The characteristics of the dolomite dissolution rate are analyzed, four stages of specimen dissolution are proposed, and the dissolution time scale is defined. Further, the characteristics of dissolution rate and pH stable acid consumption at different pH values, uniaxial compressive strength damage law, and strength damage process are studied. Through the study of the mesoscopic structure of dolomite before and after dissolution, i.e., the variation law of the mesoscopic parameters, the relationship between the pore development characteristics and dissolution time are obtained, and they correspond to the macroscopic characteristics of the sample. These results have important reference significance for the study of dolomite and have important guiding value for engineering in karst environments.

2. Materials and Methods

2.1. Test materials

The study area is located in the plateau region of Yunnan Province, in the eastern Yunnan platform fold belt of the Yangtze quasi-platform. Influenced by the Himalayan movement and neotectonic movement, the strong uplift and decline of the crust are relatively large, the gully is cut deeply, and the terrain elevation difference is very large. It belongs to the tectonic-dissolution and denudation type of low mountain landform. The test sample is the silty dolomite of the Doushantuo Formation of Sinian system (Figure 1), which is a kind of sedimentary carbonate rock mainly composed of dolomite, and small amounts of with quartz, feldspar, calcite and clay minerals. The samples were mainly composed of two types. One was the thin-section samples with lengths, widths, and heights of 60 mm × 20 mm × 5 mm, respectively, used for the initial chemical corrosion test to obtain the preliminary corrosion law and characteristics. The other was a cylindrical sample with a diameter of 50 mm and height of 100 mm, which was used for the uniaxial compressive strength test before and after dissolution (Figure 2). Before the experiment, the defective samples were removed, and rock samples with good homogeneity were selected using acoustic wave velocity tests. The end face of the sample was perpendicular to the axis of the sample, and the flatness of the end face on both sides was less

Preprints (www.preprints.org) | NOT PEER-REVIEWED | Posted: 5 September 2022 doi:10.20944/preprints202209.0052.v1

than 0.05 mm, which meets the flatness requirements. The water-rock interaction of dolomite in the study area was mainly due to chemical dissolution. Water quality analysis showed that the anions in the aqueous solution in the study area were mainly SO_4^{2-}. Using a sulfuric acid solution with low concentration, solutions with different pH values were prepared for the dissolution reaction.

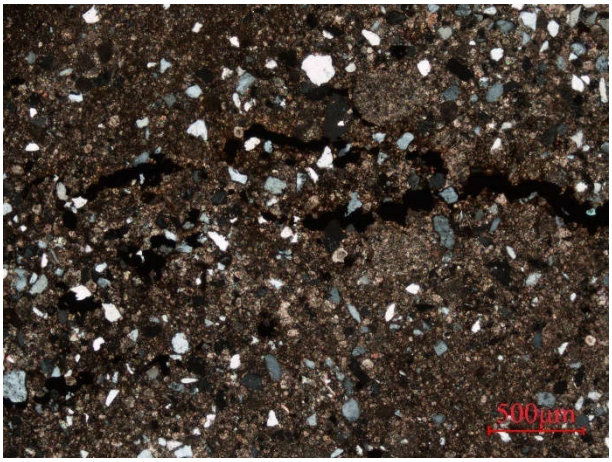

Figure 1. Image of the thin-slice dolomite under orthogonal polarization.

Figure 2. Compressive strength of the test specimen.

2.2. Chemical dissolution test of dolomite

First, the thin section sample was dried to measure its initial quality and added to different acidic solutions (pH: 1, 2, 3, 4, 5, and 7). Since the dissolution rate was high in the early stage, it was removed for drying every 1 h at first and washed and dried every 6 h after 5 h to measure its post-dissolution quality. The dissolution rate was obtained according to equation (1).

$$v_r = \frac{m_1 - m_2}{s \times t}, \quad (1)$$

where m_1 is the mass of the sample before the dissolution test, m_2 is the mass of the rock sample after the dissolution test, s is the surface area of the rock sample, and t is the dissolution time.

Additionally, the change in the pH of the solution was monitored to obtain a preliminary dissolution environment. The small sample reduced the consumption of acid, facilitated the control of the test, enhanced the accuracy of the test, and provided a basis for the dissolution environment of the mechanical specimen. Thereafter, based on the thin-slice dissolution test, the dissolution environment of the mechanical sample was determined according to the specific surface area of the sample, such as the volume of acid

Preprints (www.preprints.org) | NOT PEER-REVIEWED | Posted: 5 September 2022 doi:10.20944/preprints202209.0052.v1

solution added during dissolution. Afterward, the dissolution test of the mechanical sample was conducted with the same steps as the thin-slice sample, and the monitoring interval was changed to 3, 7, 14, and 21 days.

2.3. Uniaxial compression test

To study the strength and deformation characteristics of dolomite under uniaxial compression at different pH values and soaking times, uniaxial compression tests were carried out on the sample that was not dissolved and the samples that were dissolved for 3, 7, 14, and 21 days at different pH values. The loading method was adopted until the specimens were broken, and the loading rate was 0.1 mm/min, To reduce the test error, for each group of three specimens, the test results were taken as the median value (see Figure 3 for the test instrument).

Figure 3. Uniaxial compression apparatus.

2.4. SEM test and pore structure analysis

To study the mesoscopic mechanism of dolomite dissolution, an SEM was used to scan the undissolved sample and the sample corroded for 3, 7, 14, and 21 days at different pH values and different magnifications (Figure 4). The scanned images were analyzed using PCAS [23].

Figure 4. Scanning electron microscope (SEM).

The PCAS is based on the global threshold method and is capable of identifying a wide range of particles and pores. Binarization images (Yan et al. [24]) can eliminate useless points, segment and identify pores, and output the geometric parameters and statistical data of pores. PCAS can correct the recognition of pores by corroding the image, eliminating the influence of small joints between pores that are mistaken for new pores,

Preprints (www.preprints.org) | NOT PEER-REVIEWED | Posted: 5 September 2022 doi:10.20944/preprints202209.0052.v1

and obtaining the real pores. Figure 5 introduces the specific process of pore identification [23].

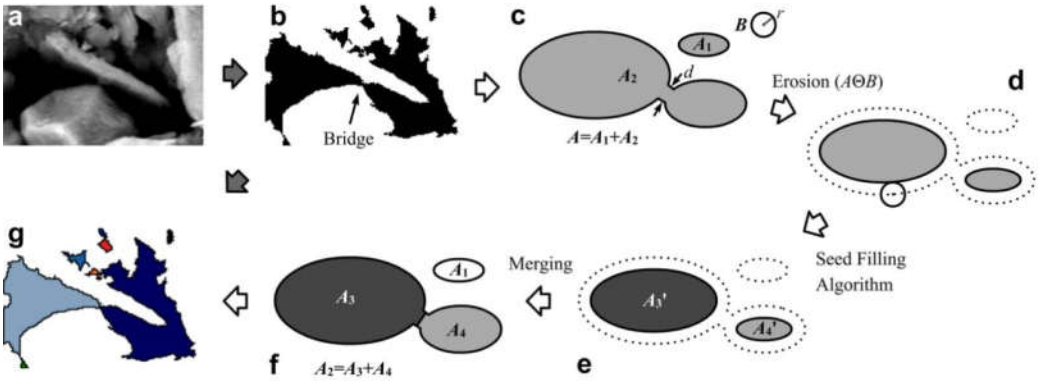

Figure 5. Pore system identification process.

3. Results

3.1. Results of dolomite dissolution

During the experiment, it was found that the dissolution of powder crystal dolomite at different pH values produced bubbles; the lower the pH, the denser the bubbles, and the more bubbles are present. A layer of argillaceous material was attached to the surface of the sample, and the argillaceous material filled by the sample was further widened. The dissolution rates of the thin-section samples at different pH values are listed in Table 1. Through the study of chemical reaction conditions with experimental phenomena, it was concluded that when pH ≤ 3, chemical dissolution is mainly based on the following formula:

$$CaMg(CO_3)_2 + 4H^+ = Ca^{2+} + Mg^{2+} + 2H_2O + 2CO_2. \quad (2)$$

When pH > 3, chemical dissolution is divided into the following two steps, and the first step reaction is the mainstay.

$$CaMg(CO_3)_2 + 2H^+ = Ca^{2+} + Mg^{2+} + 2HCO_3^-, \quad (3)$$

$$HCO_3^- + H^+ = H_2O + CO_2. \quad (4)$$

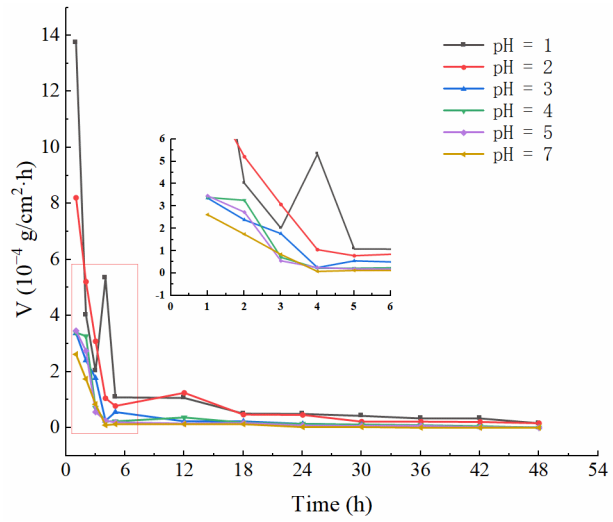

Figure 6. Dissolution rates at different pH v (10^{-4} g/cm^2·h)

Preprints (www.preprints.org) | NOT PEER-REVIEWED | Posted: 5 September 2022 doi:10.20944/preprints202209.0052.v1

According to the table content, under different pH conditions, the dissolution rate was stable after 24h, and the indoor dissolution test was divided into the initiation dissolution stage (T_1), secondary dissolution acceleration phase (T_2), dissolution equilibrium phase (T_3), and dissolution attenuation phase (T_4). The dissolution rate curve plotted by Hu Xiangbo [25] in his study of the characteristics and mechanism of deep dolomite karst sanding on the bank slope of the Meigu River Pingtou hydropower station showed a similar trend.

Although Feng et al. [7] proposed a pH damage formula that can predict the loss of acid solution during dissolution, different rocks, specimen sizes, types, and volumes of acid solutions affect the consumption of acid solutions. Therefore, it was necessary to explore the mechanical damage of rock under different pH values and control the pH within a specific range. Using the results of the chemical dissolution of the sample, the above influencing factors were determined, and a mechanical test was carried out. The strength characteristics were explored and used to determine the success of the test. Through reaction equations (2), (3), and (4), the acid consumption when pH ≤ 3 was deduced as equation (5); when pH > 3, the acid consumption is equation (6). V is acid consumption, $\gamma m'$ is the mass loss rate (its value is related to lithology and sample surface area, measured by the test), and T is the stable time required for the test, concluded in Table 1 at different pH values for the acid consumption.

$$V_1 = \frac{0.942\gamma'_m T}{10^{-pH}}, \tag{5}$$

$$V_2 = \frac{0.628\gamma'_m T}{10^{-pH}}. \tag{6}$$

Table 1. Acid consumption at different pH values

pH	Mass damage rate/(moL/h)	Settling time/h	Dosage of sulfuric acid/mL	Actual pH stabilization range
1	0.133	24	30	1–1.52
2	0.088	24	200	2–2.48
3	0.019	24	430	3–3.49
4	0.032	1	200	4–4.34
5	0.003	1	200	5–5.37

3.2. Uniaxial compressive strength of dolomite

Under the dissolution condition of pH = 1, after the uniaxial compressive strength test on the specimen, the specimen was found to be destroyed along several fissures after 3 days. When the fracture was further developed after 7 days of dissolution, the specimen was destroyed along multiple fissures. After 14 days of dissolution, multiple fissures were developed through internal fissures, and the specimen was relatively broken. Further, the fissure was developed after 21 days of dissolution, and the specimen was considerably fragmented.

Preprints (www.preprints.org) | NOT PEER-REVIEWED | Posted: 5 September 2022 doi:10.20944/preprints202209.0052.v1

(a) (b)

(c) (d)

Figure 7. Characteristic morphology of the macroscopic destruction of rocks; (a) dissolution for 3 days; (b) dissolution for 7 days; (c) dissolution for 14 days; (d) dissolution for 21 days.

Figure 8 shows that the strength of the sample gradually decreases with the increase in dissolution time. This was because the pores of the fine sample were significantly developed by dissolution, and the crack expansion increased. Some cemented materials were separated from the parent rock, making the rock structure loose, thereby decreasing the strength. Figure 9 shows that the more acidic the rock sample, the faster the strength decreases. At pH = 1, under the condition of the same dissolution for 3 days, the strength decrease rate of the sample was 31.8%, which was 7.95 times that of the rock strength decrease rate at pH = 7. At 21 days of dissolution, the strength decrease rate of rock was 76.2%, which was 2.39 times that of 3 days of dissolution.

Preprints (www.preprints.org) | NOT PEER-REVIEWED | Posted: 5 September 2022 doi:10.20944/preprints202209.0052.v1

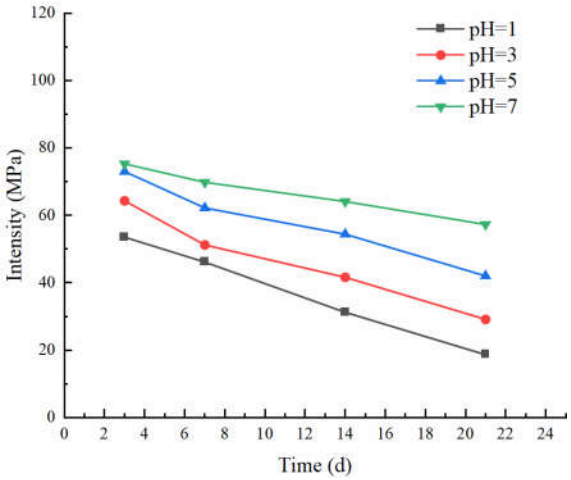

Figure 8. Relationship curves between dolomite strength and soaking time at different acidity levels.

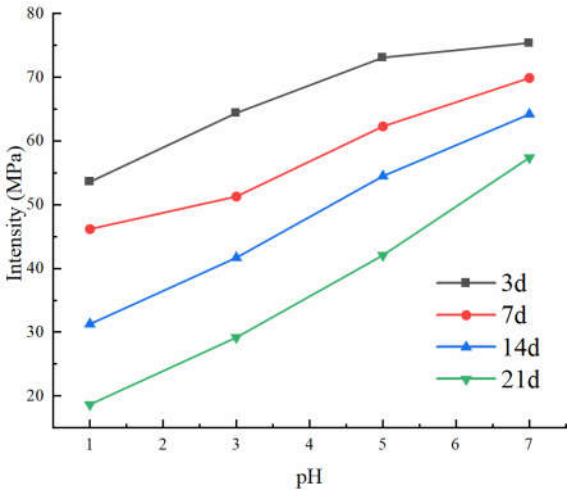

Figure 9. Relationship curve between dolomite intensity and acidity at different times.

3.3. Microstructure of dolomite

During the dissolution of dolomite, the internal structure changed, which significantly affected the parameters, such as dolomite strength. Both the surface and fresh section of the specimen were scanned by electron microscopy, which observed the surface dissolution and internal dissolution. At the end of the corrosion test, only the SEM images of the surface of the corrosion samples at different pH values were analyzed because of the lack of an obvious corrosion effect on the cross-section. (See Figure 10).

Preprints (www.preprints.org) | NOT PEER-REVIEWED | Posted: 5 September 2022 doi:10.20944/preprints202209.0052.v1

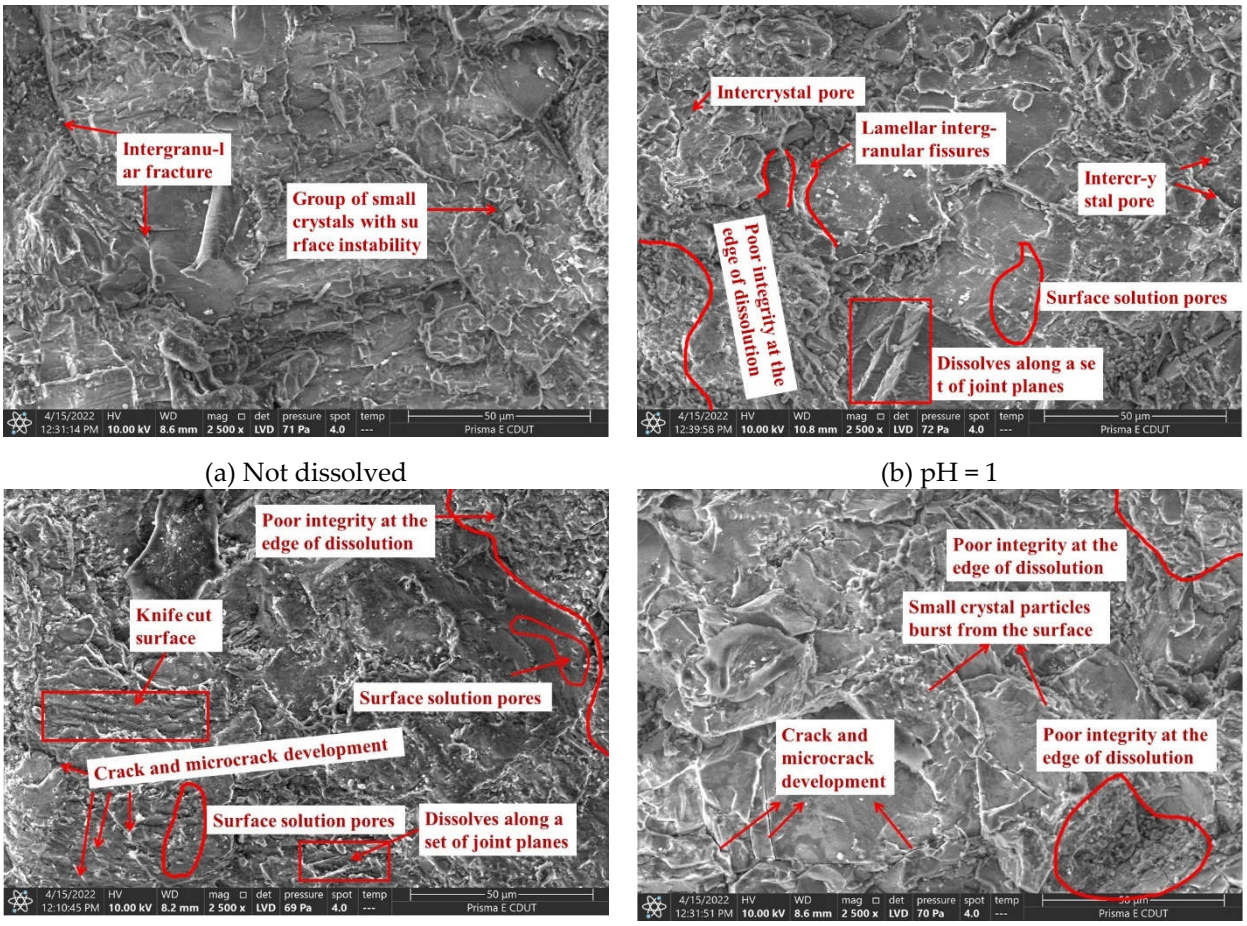

Figure 10. SEM images of the samples at different pH values.

The SEM image shows that the lower the pH, the more the pore fissures develop, and the weaker the adhesion between the particles, which gradually collapse into relatively small particles, and this is different from the result obtained by Weng [26]. The overall karst action of dolomite is divided into processes, such as osmosis, dissolution decomposition, and mechanical disintegration, and the dolomite powder is generated on the surface of the specimen during dissolution. This further confirmed that dolomite is mainly dissolved along the intergranular pore or crystal binding surface, and the crystal shedding during the dissolution process is often accompanied by the shedding of the crystals to form dolomite powder. However, some specimens did not contain dolomite powder, or dolomite powder was considerably small, because the clay minerals contained in the sample during dissolution wrapped the dolomite crystal on the surface or inside, making it difficult for the crystal to break away from the parent rock. According to the image, it was observed that the dissolution of the dolomite was more prominent in its edge dissolution because the amount of H^+ adsorbed at the edge of the rock mass was significantly high and the reaction was considerably sufficient. The dolomite in the study area exhibited unique mesoscopic dissolution characteristics, i.e., it is dissolved along a set of joint surfaces to produce a mesoscopic fault structure. Thus, the strength of the dolomite in the study area was lower than that of the dolomites in other regions. Further, when the acidity was high, pores were mainly developed, and the knife-shaped surface was consistent with the actual situation. When the acidity was low, cracks were mainly developed.

Preprints (www.preprints.org) | NOT PEER-REVIEWED | Posted: 5 September 2022 doi:10.20944/preprints202209.0052.v1

4. Discussion

4.1. Dolomite dissolution phases

T_1 occurred at the beginning of dissolution, and because the rock surface was fresh, the initial reaction rate was considerably high. However, as the dissolution progressed, the dissolution products attached to the surface, preventing the reaction from proceeding. T_2 occurred after T_1. The dissolution products attached to the surface of the specimen were and the newly developed pores increased the contact area, exposing more fresh rock samples and gradually washed away, showing the characteristics of secondary acceleration. T_3 occurred after T_2, that is, the newly developed pores were reattached to the dissolution products, and even if they were rinsed, there were almost no newly developed contact surfaces, and the dissolution was stable. T_4 occurred after T_3; the dissolution rate was stable, the fluctuation was small, and it had similar characteristics to the actual dissolution environment. In the dissolution environment of pH = 1, the dissolution rate images of each dissolution stage were drawn (see Figure. 10).

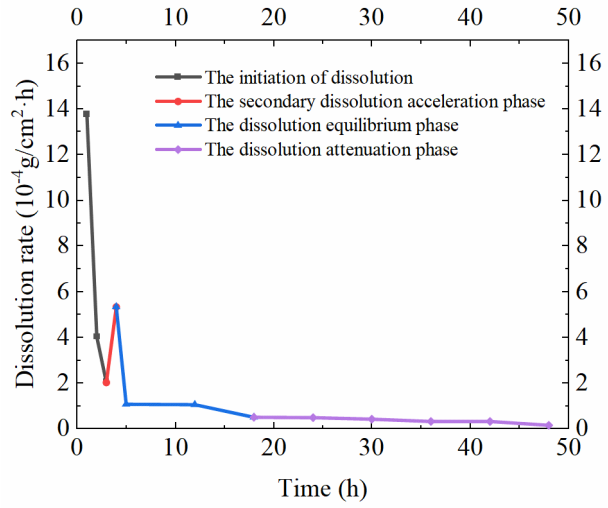

Figure 11. Division of indoor dissolution stages.

4.2. Time-dependence of dolomite dissolution

By calculating the average dissolution rate of each of the four stages and combining the chemical reaction rate parameters, the dissolution time-scale relationship at different pH values was obtained. Short-term simulation can save time, facilitate control, and effectively reduce the impact of parameter changes, such as temperature, in the process.

Zhou [27] defined the concept of dissolution time scale from the perspective of reactant consumption. This definition of the dissolution time scale λ can reflect the number of days of indoor dissolution, which is equivalent to on-site dissolution. Table 2 shows the average dissolution rates at different pH values. The experimental dissolution environment was assumed to be pH = 1, the engineering environment was pH = 7, and v_r is the average dissolution rate. In equation 8, λ_1 is the time scale for starting the dissolution phase, T11 is the time for starting the dissolution stage when pH = 1, and the subsequent corner indices are the same.

$$\lambda = \frac{T_x}{T_0}, \tag{7}$$

$$\lambda = \lambda_1 T_{11} + \lambda_2 T_{12} + \lambda_3 T_{13} + \lambda_0 T_{10}. \tag{8}$$

Preprints (www.preprints.org) | NOT PEER-REVIEWED | Posted: 5 September 2022 doi:10.20944/preprints202209.0052.v1

Table 2. Time scale of dissolution stages.

Dissolution rate (T_x)	pH = 1 (v_r)	pH = 7 (v_r)	Time scale of dissolution (λ)	Dissolution time (T_{1x})
Initiate the dissolution phase (T_1)	6.603	1.328	4.972	3
Accelerated phase of secondary dissolution (T_2)	3.685	0.114	32.325	1
Dissolution equilibrium phase (T_3)	0.572	0.133	4.301	14
Dissolution attenuation phase (T_4)	0.502	0.082	6.122	6

From the lambda value, it was found that one day of dissolution at pH =1 was equivalent to 144.187 days of dissolution at pH = 7 in the project, and this is the time scale. The dissolution characteristics of the study area were simulated in a short time, which provides an important basis for actual engineering.

4.3. Macroscopic destruction of dolomite

To further explore the mechanical strength damage characteristics of dolomite under the dissolution, the stress–strain curves of the various stages of dolomite dissolution at different pH values were plotted (Figure 12). For the undissolved dolomite, when 75%–85% of the peak strength of the rock sample was loaded, the rock sample produced cracks along the compressive stress direction. When the peak strength was reached, there was a loud noise, and the sample strength decreased in a very short time. The sample was brittle and failed mainly along the cracks. When the dissolution time exceeded 7 days, the loading time of the sample to the peak strength and the time from the peak strength to the loss of strength gradually increased. Further, the failure strain increased, which was due to the increased development of pore cracks in the sample and the increased distribution density; the range increased, the flexibility of the sample was enhanced, the sound at the time of destruction was gradually reduced, and the sample was considerably broken after the destruction.

Preprints (www.preprints.org) | NOT PEER-REVIEWED | Posted: 5 September 2022 doi:10.20944/preprints202209.0052.v1

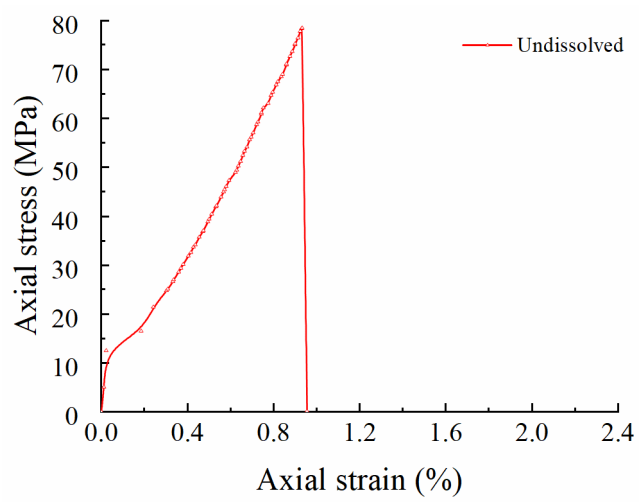

(a) Stress–strain curve of unsolved dolomite

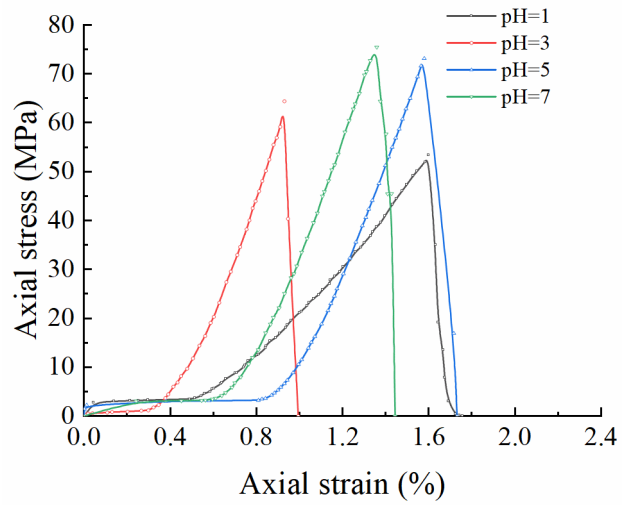

(b) Stress–strain curves of dolomite after dissolution for 3 days

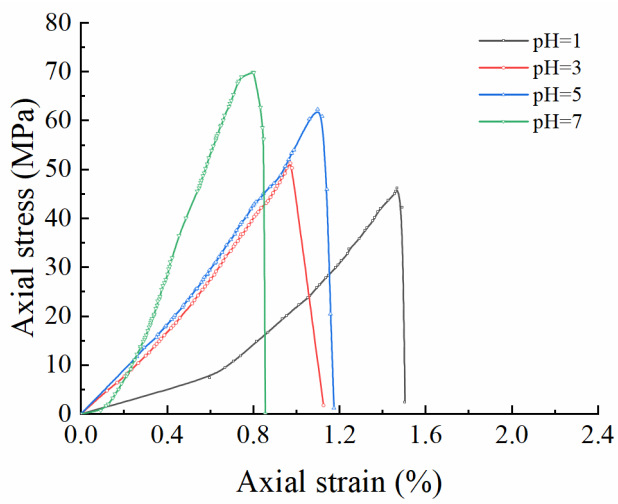

(c) Stress–strain curves of dolomite during 7 days of the dissolution

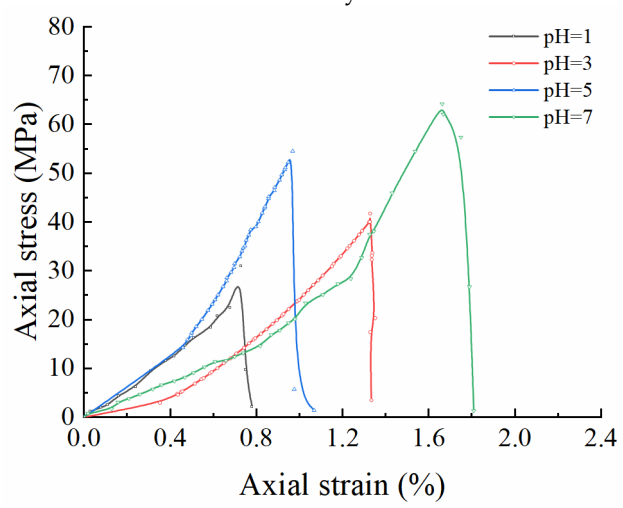

(d) Stress–strain curves of dolomite after 14 days of the dissolution

Figure 12. Stress–strain curves of dolomite at different dissolution stages and different pH values.

4.4. Dissolution evolution of dolomite Microstructure

After the sample was processed using an SEM, the microscopic changes of the sample before and after the dissolution was observed in the image, but only through qualitative analysis. Using PCAS software, the structural characteristics, such as porosity, pore size, shape factor, fractal dimension, and probabilistic entropy, before and after dissolution were quantitatively analyzed. Further, the dissolution condition of pH = 1 was used to study the powder dolomite dissolution characteristics (Table 3).

Preprints (www.preprints.org) | NOT PEER-REVIEWED | Posted: 5 September 2022 doi:10.20944/preprints202209.0052.v1

Table 3. Pore characteristics of samples at different dissolution days.

parameter	3 days	7 days	14 days	21 days
Total number of holes	383	908	1182	5374
Porosity/%	8.38	12.32	14.56	19.28
Maximum area/μm²	0.7461	0.5761	0.5660	0.5116
Average area/μm²	0.0854	0.0751	0.0383	0.0324
Average perimeter/nm	229.11	116.98	110.34	41.1
shape factor	0.5463	0.3561	0.3513	0.2695
Maximum length/nm	368.76	195.55	164.5	152.92
Average length/nm	55.48	33.46	32.27	14.13
Maximum width/nm	107.82	94.67	91.01	80.66
Average width/nm	29.78	19.25	17.44	7.75
Probabilistic entropy	0.9807	0.9754	0.9745	0.9673
Fractal dimension	1.7366	1.3971	1.3272	1.2005

As the dissolution progressed, the pore development eventually reached 19.28%, which was 2.3 times that of the initial dissolution, and the porosity increase rate was 0.6%/d, the average perimeter decrease rate of pores was 10.4 nm/d, and the increase rate of the pore number was 277.3/d. This showed that the pores developed from a small number of large pores to a large number of micropores; however, the aspect ratio of the pores was maintained at approximately 1.7–1.85, indicating that the pores developed at a similar rate in different directions.

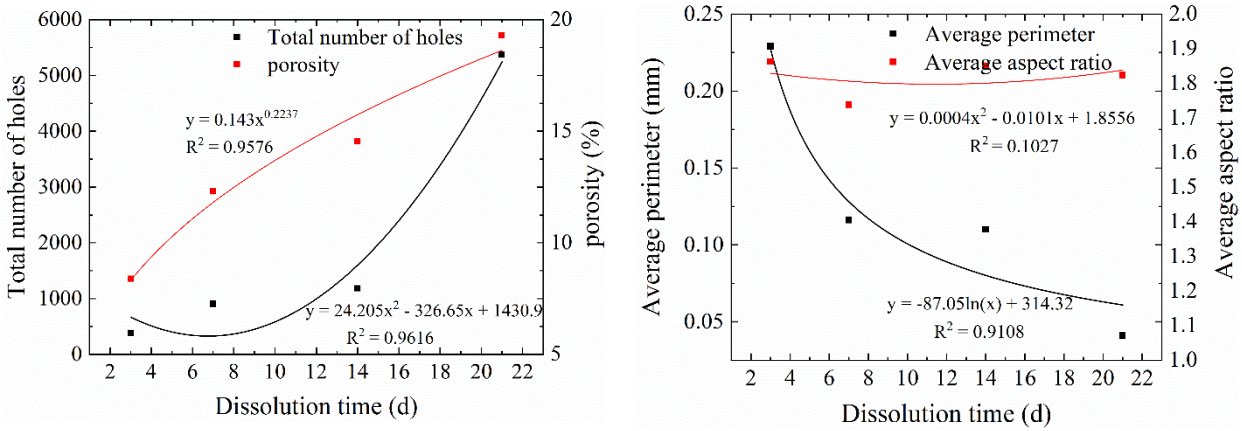

(a) (b)

Figure 13. Effect of dissolution time on the pore parameters of dolomite.

5. Conclusions

(1) The indoor dissolution characteristics of dolomite, such as dissolution rates at different pH values, acid consumption of samples at different pH values, four dissolution stages, and the approximate dissolution time scale between dolomite and the engineering environment were determined by experiments.

(2) Under different pH conditions and dissolution days, with an increase in acidity and dissolution time, the macroscopic mechanical characteristics of the sample changed from brittle to flexible, and the time to reach peak strength and the time from peak strength to complete loss of strength increased. Additionally, the strength damage rate at different pH values and dissolution days was 4%–76.2%.

(3) SEM showed that the dolomite in the study area developed more pores and fractures with dissolution. Further, the bond between the particles was weak, and the particles gradually collapsed into relatively small particles, which was consistent with the overall karst process of dolomite, including osmosis, dissolution, decomposition, and mechanical disintegration. Additionally, it exhibited dissolution characteristics along the joint plane and generated a knife-shaped surface, which corresponded to macroscopic dissolution

characteristics. Further, the edge of the sample was more obvious, which is related to the enrichment of H^+.

(4) SEM images were used to analyze the microscopic structure of the samples after dissolution. It was found that with the dissolution process, the final pore development was 19.28%, which was 2.3 times more than the initial dissolution. The pore growth rate was 0.6%/day, the average pore circumference decrease rate was 10.4 nm/day, and the pore number increase rate was 277.3/day. The pores were considerably developed; however, the length to width ratio of the pores was maintained at approximately 1.7–1.85, indicating that the pores develop at similar rates in different directions.

(5) The dissolution time scale of this test was based on different acidities, and the dissolution time scale can be defined according to the specific gravity of different dissolution stages under the same acidity.

(6) The evolution of the microstructure under different acidities and dissolution times in the same area can be studied.

Author Contributions: Conceptualization, W.L.; writing, P.L; resources, H.X.; investigation, B.G.; methodology, F.J.; All authors have read and agreed to the published version of the manuscript.

Funding: This research received no external funding.

Acknowledgments: The valuable comments made by the anonymous reviewers are sincerely appreciated.

Conflicts of Interest: The authors declare no conflict of interest.

References

1. Wang, Z.J.; Du, Y.W.; Jiang, Y.F.; Wu, F.; Qi, Y.L.; Zhou, P. Study on the destabilization mechanism of tunnel palm faces in sandy dolomite strata. *J Rock Mech Eng*. **2021**, *40* (supp. 2), 3118–3126.
2. Yu, S. Study on engineering characteristics of karsted dolomite. *West Prospect Proj*. **2013**, *25*, 139–140.
3. Zhang, Z.Q. Study on mechanical properties of sandy dolomite with different moisture content. *Sci Technol Innov*. **2022,** *04*, 79–82.
4. Wiederhorn, S.M.; Johnson, H. Effect of Electrolyte pH on Crack. Propagation in Glass. *JAmCeramSoc,**1973**,56:192-197*.
5. Atkinson, B.K.; Meredith, P.G. Stress corrosion cracking of quartz: A note on the influence of chemical environment. *Tectonophysics*. **1981**, *7*, 1–1.
6. Tang, L.S.; Wang, S.J. Discussion on mechanism and quantification method of chemical damage of rock water. *J Rock Mech Eng*. **2002**, *03*, 314–319.
7. Feng, X.W.; Wang, W.; Wang, R.B.; Yuan, S.S.; Zhu, Q.Z. Ontogenetic model of rheological damage in sandstone considering water chemical damage. *Geotech Mech*. **2018**, *39*, 3340–3346 + 3354.
8. Cui, Z.A.; Bao, Z.Y.; Zhang, T.F.; Dong, Z.C. Experimental study on dissolution kinetics of carbonate rocks under burial conditions. *J Oil Gas Technol*. **2007**, *29*, 204–207.
9. Huang, K.J.; Wang, W.; Bao, Z.Y.; Xie, S.Y.; Wan, N.; Mei, L.F.; Qian, Y.X. Dissolution modification of the Feixianguan Formation reservoir in the northeastern Sichuan Basin by buried organic acidic fluids: an experimental study of dissolution kinetics. *Geochemical*. **2011**, *40*, 289–300.
10. Xie, S.Y.; Shao, J.F.; Xu, W.Y. Influences of chemical degradation on mechanical behaviour of a limestone. *Int J Rock Mech Min Sci*. **2011**, *48*, 741–747. DOI:10.1016/j.ijrmms.2011.04.015.
11. Yurtdas, I.; Xie, S.Y.; Burlion, N.; Shao, J.F.; Saint-Marc, J.; Garnier, A. Influence of chemical degradation on mechanical behavior of a petroleum cement paste. *Cem Concr Res*. **2011**, *41*, 412–421. DOI:10.1016/j.cemconres.2011.01.008.
12. Li, G.L.; Wei, L.Y.; Jin, H.W.;Su, H.J.; Zhang, T.; Li, M. Experimental study of dynamic compressive mechanical properties of tuffs after acid corrosion. *Rock Soil Mech*. **2017**, *38*, 3247–3254.
13. Wang, W.; Liu, T.G.; Lv, J.; Wang, R.B; Yuan, S.S; Zhu, Q.Z. Experimental study of influence of water-rock chemical interaction on mechanical characteristics of sandstone. *Chin J Rock Mech Eng*. **2012**, *31* (supp. 2), 3608–3617.
14. Deng, H.F.; Hu, A.L.; Li, J.L.; Zhang, X.J.; Hu, Y.; Chang, D.L.; Zhu, M. Statistical constitutive model of sandstone degradation damage under water-rock interaction. *Rock Soil Mech*. **2017**, *38*, 631–639. DOI:10.16285/j.rsm.2017.03.003.
15. Chen, S.L.; Feng, X.T.; Zhou, H. Sandstone triaxial microscopic damage mechanism and damage variable analysis under chemical corrosion. *Rock Soil Mech*. **2004**, *09*, 1363–1367.
16. Pokrovsky, O.S.; Golubev, S.V.; Schott, J. Dissolution kinetics of calcite, dolomite and magnesite at 25 Â°C and 0 to 50 atm pCO_2. *Chem Geol*. **2005**, *217*, (239–255). DOI:10.1016/j.chemgeo.2004.12.012.
17. Sun, Y.P.; Wei, L.N.; Dai, C.L.; Yu, Z.H.; Xin, Y. The carbonic acid-rock reaction in feldspar/dolomite-rich tightsand and its impact on CO_2-water relative permeability during geological carbon storage. *Chem Geol*. **2021**, *584*. DOI:10.1016/j.chemgeo.2021.120527.

18. Yang, Y.K.; Liu, B.; Qin, S.; Luo, P; Zhang, D.M; Zhou, M.H; Shi, K.B; Tian, Y.J. Re-recognition of deep carbonate dissolution based on the observation of in-situ simulation experiment. *Acta Sci Nat Univ Pekinensis*. **2014**, *50*, 316–322.
19. Chun, Z.; Xiao, D.; Xu, W.R.; Liu, F.X.; Yun, L. Chen C,Xue L. Softening damage analysis of gypsum rock with water immersion time based on laboratory experiment. *IEEE Access*. **2019**, *0006*, 7.
20. Laurent, E.; Krassimira, M.; Franci, G.; Wolfgang, D. The inhibiting action of intrinsic impurities in natural calcium carbonate minerals to their dissolution kinetics in aqueous H_2O-CO_2 solutions. *Geochim Cosmochim Acta*. **1999**, *63*, 989–1002.
21. Kuva, J.; Sammaljärvi, J.; Parkkonen, J.; Siitari-Kauppi, M.; Lehtonen, M.; Turpeinen, T.; Timonen, J.; Voutilainen, M. Imaging connected porosity of crystalline rock by contrast agent-aided X-ray microtomography and scanning electron microscopy. *J Microsc*. **2018**, *270*, 98–109. DOI:10.1111/jmi.12661.
22. She, M.; Shou, J.F.; Shen, A.J.; Pan, L.Y.; Hu, A.P.; Hu, Y.Y. Experimental study on dissolution law and pore evolution of carbonate rocks. *Oeil Explor Dev*. **2016**, *43*, 564–572.
23. Liu, C.; Shi, B.; Zhou, J.; Tang, C. Quantification and characterization of microporosity by image processing geometric measurement and statistical methods: Application on SEM images of clay materials. *Appl Clay Sci*. **2011**, *54*, 97–106. DOI:10.1016/j.clay.2011.07.022.
24. Yan, G.Y.; Wei, Z.T.; Song, Y.; Zhang, J.J.; Yang, H. Quantitative characterization of shale pore structure based on Ar-SEM and PCAS. *Geoscience*. **2018**, *43*, 1602–1610.
25. Hu, X.B. Study on the Characteristics and Mechanism of Karst Sandyization of Dolomite in Pingtou Hydropower Station on Meigu River [D]; *Chengdu University of Technology*, 2009.
26. Weng, J.T. Differential dissolution of calcite and dolomite. *Karst China*. **1984**, *01*, 31–40 + 107–108.
27. Zhou, J.F. Study on rock soaking time scale and degradation prediction model under acidic solution. *Water Conserv Hydropower Technol (English andChinese)*. **2021**, *52*, 162–171.